Experimental research on flow field in the draft tube of pump turbines based on LDV

Experimental research on flow field in the draft tube of pump turbines based on LDV

D M Liu[1,2], Y Z Zhao[2] and Z G Zuo[1]
[1]State Key Laboratory of Hydro Science & Hydraulic Engineering, Beijing 100084, China
[2]Research & Development Center of Dongfang Electric Machinery CO., LTD, Deyang, 618000, Sichuan Province, P.R. China.

E-mail: liudemin999@126.com

Abstract. A large number of pumped storage power plants will be put into operation in China. The current development of modern pump storage power plants aims towards a higher flexibility and stability in operation, and an extended operation range of the hydraulic machine. These projects have a large number of problems. For problems of the turbine units, the optimization of pump turbine is very crucial to ensure the unit's high efficiency and stability. The velocity distribution on the runner outlet is very important to optimize the pump turbine. In this paper, the velocity on runner outlet was tested by LDV (Laser Doppler Velocimetry). The axial velocity and circumferential velocity on runner outlet were tested at different working points by LDV. The velocity distribution can provide important reference for the runner design.

1. Introduction

All over the world, the production of energy by renewable sources such as wind and solar is increasing massively. In order to absorb more and more intermittent renewable energy in a given network, complementary power sources with high flexibility are needed. Among them, Hydro Pumped Storage Plants (PSP) using reversible pump-turbine machines is an ideal complement, due to their fast response capability and their ability to store large amounts of potential energy.

The flexibility of pumped storage plants is a necessity during their operations. Frequent starts and stops, as well as fast mode changes are increasingly required, particularly from the pump mode to the turbine mode. Reversible pump-turbine machines need to be designed for high availability, reliability and stability, especially during the start-up process in turbine mode when peak power production is required [1].

The development tendency of pump-turbine machines in China is high rotation speed, high head, larger capacity and variable speed. The main indicators of pump-turbine are safety and stability. There are a lot of researches on the internal flow phenomena, however, only a few of them have studied the optimization of turbine geometry parameters to meet the pump-turbine safety requirements [2].

Many crucial problems such as transient process, S characteristic and pump hump phenomena are related to the flow state in the runner. The LDV is a useful tool to test the internal flow phenomena especially the velocity on draft tube [3].

The basic principle of LDV is to measure the fluid velocity in the flow field by detecting the Doppler Effect in the laser beam. When the flow fields of the particles at a certain speed by two laser beams are

intersecting, the frequency shift will happen according to the law of Doppler particle scattering of laser, and the strength of the frequency shift is proportional to the particle velocity. The velocity of the intersecting point in the flow field can be obtained by capturing and analyzing the frequency shift information of the scattered light. By measuring the velocity difference between particles, the velocity of the impeller can be measured and the image can be taken by high-speed photography [4].

The LDV test has also been applied on fluid machines such as pumps and propellers. The clear radial flow velocity vector diagram can locate the position of air separation flow in an impeller at different conditions. Secondary flow vector diagrams can display the changes of flow affected by the centrifugal force and Coriolis force in the flow [5-7]. Based on the characteristics of the propeller wake symmetry in circumferential direction, the circumferential velocity distribution of propeller wake in uniform flow is measured by 2D-LDV [8-9].

Erne [10] assessed the mean flow field and low frequency disturbances in the stay vane channel of a model pump turbine by using the transient numerical simulations and LDV-based measurements. The axial velocity and meridional velocity were tested by LDV. A shifting velocity distribution between the shroud and the hub of the distributor was obtained when continuously increasing the discharge in the part-load range during the experiment.

By means of in-stationary LDV-measurements, Zhang [11] detected the rotating stall phenomena with a significant frequency peak at 1-2Hz induced by the periodically unsteady flow.

The radial velocity component and the secondary flow component streamline velocity were tested by Braun [12]. During the operating conditions, 4 stall cells were found, and velocity was measured by LDV.

Two-component LDV was used to investigate the axial and tangential velocity fluctuations at the runner outlet of a reduced scale model of a Francis turbine. The impact of cavitation and hydro-acoustic resonance on both axial and tangential velocity fluctuations in terms of amplitude and phase shift was highlighted by Favrel [13].

The pressure-phase average evolution of the tangential and the axial velocity components C_u and C_m at a given radial position were tested by Müller [14].

Many researchers paid attention to the flow phenomena especially the vortex separation on fluid machines. For hydro-turbines, the vortex is the source of fluid machinery vibration. If the cause of vortex separation can be found, the cause of vibration will be found.

Wang, Magnolia, Liu and Yin [15-18] presented the experiment and simulation results of a pump-turbine operating at off-design conditions in the turbine mode. The main flow at the off-design conditions was dominated by one stall vortex rotating with the impeller at sub-synchronous speed in the vane-less space between the impeller and guide vanes. It was likely the result of flow separations developed in several consecutive impeller channels, which lead to their blockage.

In this paper, the velocity on draft tube was tested at different working points, the best efficiency working point, the high pressure fluctuation amplitude working point and pump slope zone.

2. Experiment

2.1 LDV test on pump-turbine

The research object is a reduced pump-turbine, and the whole model includes the draft tube, runner, guide vane, stay vane and spiral case, as shown in Figure 1. The number of runner blades is 9 and the number of guide vanes is 20, as listed in Table 1.

The main test instruments include LDV laser, high speed camera, and light source and so on, as shown in Figure 2. The LDV laser was arranged on $1D_2$ of the draft tube. The velocity was tested by the Fluorescent particles scatting which were injected from the draft tube in water. Two acrylic windows installed in the draft tube can provide optical access to the flow region of interest. The surfaces of the acrylic windows were machined plane-parallel for easier positioning of the LDV laser beam intersections.

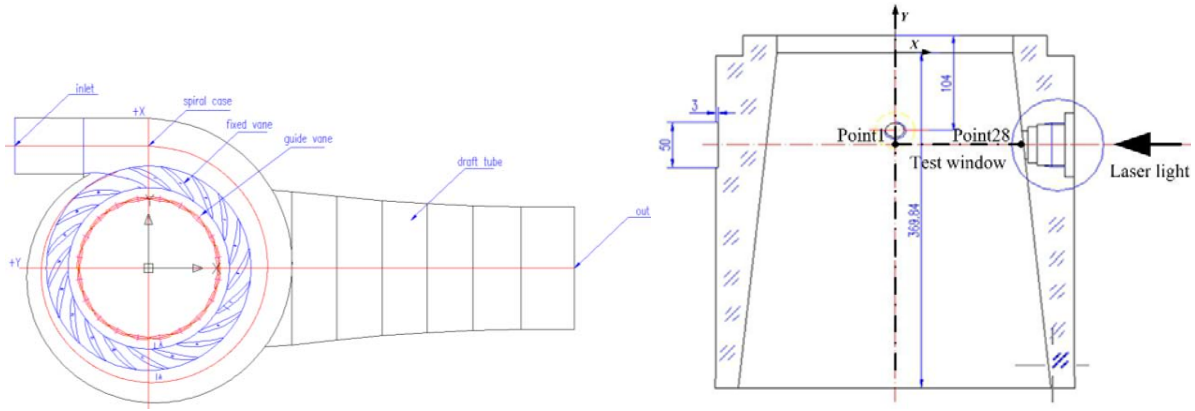

(a) Flow passage (turbine mode) (b) Flow passage (turbine mode)

Figure 1. The structure of the pump-turbine model.

Table 1. Main parameters of the tested pump-turbine model.

Runner diameter at inlet (mm)	513
Runner diameter at outlet (mm)	300
Runner blade number Z_1	9
Guide vane number Z_0	20
Maximum guide vane opening a (°)	24
Rotational speed (rpm)	1100
Height of guide vane (mm)	57.2

Figure 2. The LDV test of reduced pump-turbine.

The intersection of the beams was positioned at the defined monitoring points using a 2-axis traverse system controlled by the LDV data acquisition software Flowsizer. The transparent test window was flat to reduce the refraction of light, as shown in Figure 3. The two test windows had flat surfaces with 3mm thickness and 45mm diameter. Both the inside and lateral surfaces were flat. The laser light was perpendicular to the flat surface and the light entered the test window along the +X direction across the

flat surface in Figure 1. In this way, the index of refraction of the flat surface is smaller than that of the cylindrical surface.

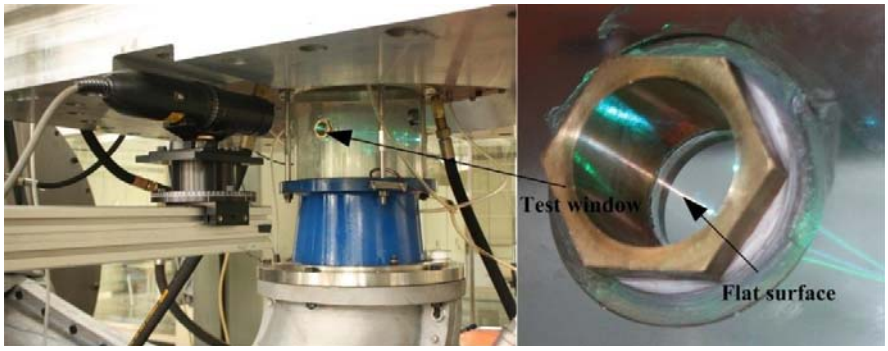

Figure 3. The test window of reduced pump-turbine.

The main performance parameters of LDV are shown in Table 2.

Table 2. Key parameters of LDV instruments.

Parameters	Values
Velocity range *V* (m/s)	-150-1000
Sampling frequency *f* (MHz)	400-800
Systematic uncertainty of velocity	0.1%

For the complex flow characteristics of the flow field in the pump-turbine, the scattering and tracking abilities of the tracer particles should be. Hollow glass balls with good tracking and scattering characteristics is better than most other solid particles, because their density is close to water. The hollow glass balls with the size of 10 μm were chosen as the tracer particles. More glass balls can be captured through the flat surface window when compared with the cylindrical surface.

2.2 The parameters of test stand

The test of LDV was conducted on the DF-150 Test Stand in Dongfang Electric, as shown in Figure 4. It can perform the efficiency test, the cavitation test, and pressure fluctuation test according to the IEC 60193 standard. The key test parameters such as water head, runner diameter and rotational speed are listed in Table 3.

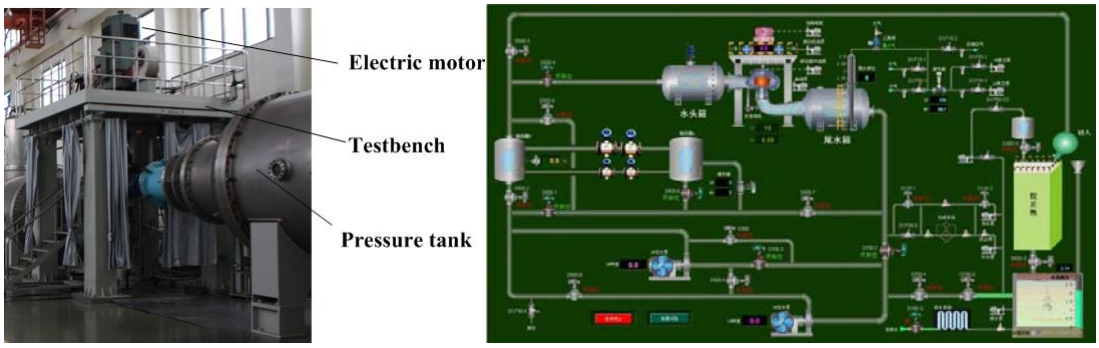

Figure 4. DF-150 test stand.

Table 3. Key parameters of DF-150 test stand.

Parameters	Values
Maximum test head H (m)	150
Model runner diameter D (mm)	250～500
Maximum speed of dynamometer N(r/min)	2500
Generator power P (kW)	500
Maximum test discharge Q (m^3/s)	1.5
Suction head of model runner H (m)	-8.5～+25
Systematic uncertainty of efficiency	±0.25%

The accuracies of key experimental parameters in the LDV test are listed in Table 4.

Table 4. Accuracies of key parameters of the LDV test.

Measuring items	Measuring instrument	Uncertainty
Discharge Q	Electromagnet flow meter	0.20%
Speed N	Speed sensor	0.02%
Head H	Pressure sensor	0.05%
Load	Load sensor	0.05%
Absolute pressure	Pressure sensor	0.10%
Pressure fluctuation	Dynamic Pressure sensor	0.10%
Water temperature	Temperature sensor	±0.10°
Air discharge	Flow meter	0.10%
Wicket gate angle	Angle displacement sensor	0.10%

3. Results and analysis

3.1 Working points

The velocity at the draft tube inlet was tested by LDV equipment. The tested working points are listed in Table 5. There were 10 working points in the turbine mode and 2 working points in the pump mode. Among these working points, the working points 1 to 5 and the working points 6 to 10 were tested at the rated head and the optimal head in the turbine mode, respectively.

Table 5. Tested working points in turbine mode of the reduced pump-turbine.

H	Working point	N/N_r (%)	Q_{11} (L/s)	n_{11} (r/min)	a (°)	H_{test} (m)	n (r/min)
H_r	1	optimal	437.00	38.78	12.60	61.19	1209.81
	2	100	605.70	38.78	18.73	59.07	1189.81
	3	80	483.87	38.78	14.23	59.66	1194.82
	4	60	372.39	38.78	10.63	60.02	1196.82
	5	40	269.37	38.78	7.68	51.24	1104.81
$H_{optimal}$	6	60	274.45	34.80	7.11	51.31	994.81
	7	80	350.63	34.80	9.14	50.64	989.95
	8	100	430.60	34.80	11.38	49.85	979.88
	9	optimal	470.00	34.80	12.60	55.91	1039.81
	10	120%*$Q_{opt.}$	564.00	34.80	15.86	55.93	1039.81

The working points 11 and 12 were tested at the maximum head and minimum head in the pump mode, respectively in Table 6.

Table 6. LDV working points in the pump mode of the reduced pump-turbine.

Working point	h	f (HZ)	φ	ψ	a (°)	H_{test} (m)	n (r/min)
11	h_{max}	50	0.25047	5.16376	14.28	54.942	1100
12	h_{min}	50	0.29788	4.79561	18.65	51.231	1100

Some variables were calculated by equation (1).

$$\varphi = \frac{240Q_m}{\pi^2 nD^3\rho} \qquad \psi = \frac{7200gh}{\pi^2 n^2 D^2} \qquad n_{11} = \frac{nD_1}{\sqrt{H}} \qquad Q_{11} = \frac{Q_m}{D_1^2\sqrt{H}} \tag{1}$$

where Q_m is the mass discharge, n is the rotational speed, D is the runner diameter, ρ is the water density, g is the gravitational speed, h is the pumping head, H_{test} is the experimental hydraulic head, N is the output power, a is the guide vane opening, h_{max} is the largest pumping head, h_{min} is the smallest pumping head, H_r is the rated head and $H_{optimal}$ is the optimal head.

3.2 Tested results

For the independency of the tested results, the axial velocity V_z on same radius position was tested continuous 10 times at the working point 1. The error analysis was checked in Figure 5(a). The velocity error on the working point 1 was small about $\pm 0.8\%$. The error analysis was checked by equation (2).

$$R = \frac{V_z - \overline{V}_z}{V_z} \times 100\% \tag{2}$$

where, $\overline{V}_z$ is the average axial velocity of continuous 10 tested results.

From the circle center to draft wall, the distance is divided 28 points in Figure 1(b). The velocity is tested at each point and the discharge $Q_{integration}$ is obtained by the velocity multiply by the area and then integration. The integral discharge is compared to the tested discharge Q_f which is obtained by flow meter. The error analysis according to Eq. (3) is obtained at each working points in Figure 5(b).

$$R = \frac{Q_{integration} - Q_f}{Q_f} \times 100\% \tag{3}$$

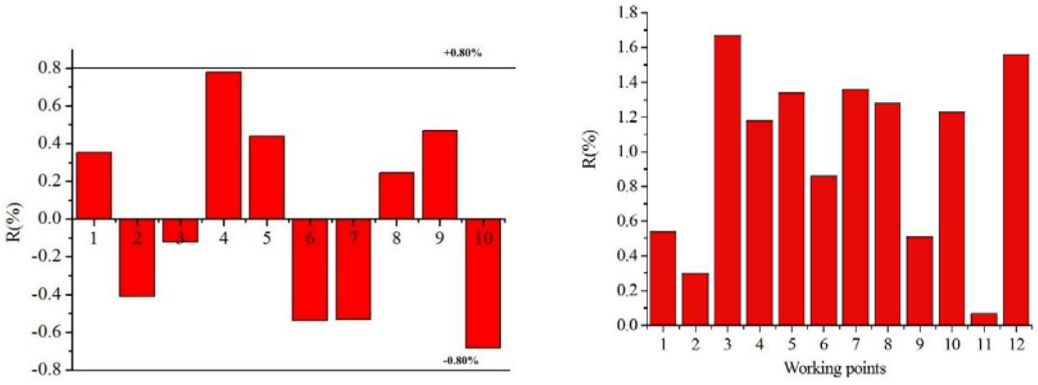

(a) Error at working point 1 (b) Error at working points 1-12

Figure 5. Error analysis at different working points.

The tested axial velocity V_z and circumferential velocity V_u of 10 working points in the turbine mode are shown in Figure 6. The error bar is shown in each curve according to the Figure 5. In the abscissa, 0 represents the center and 1 represents the side wall of the draft tube along the radial direction. At the rated head, velocity V_u at point 1 to point 4 near the center of the draft tube is higher than that near the side wall. Both axial and circumferential velocity near the center of the draft tube are positive while they are negative near the side wall, which are consistent with the design characteristics of hydraulic turbines. From the point view of velocity distribution, there is no larger backflow zone at the runner outlet from point 1 to point 4. The axial velocity is very small near the center of the draft tube at the working point 5 due to deviation from the best efficiency zone. The working points 6 to 10 are operating at the optimal head, but only working points 7 to 10 have good velocity distribution, which can be used as the reference for the optimal design. The velocity distribution at the working point 6 is not good, and the velocity near the center of the draft tube is 0, which is caused by operating close to the lower limit of the operating range.

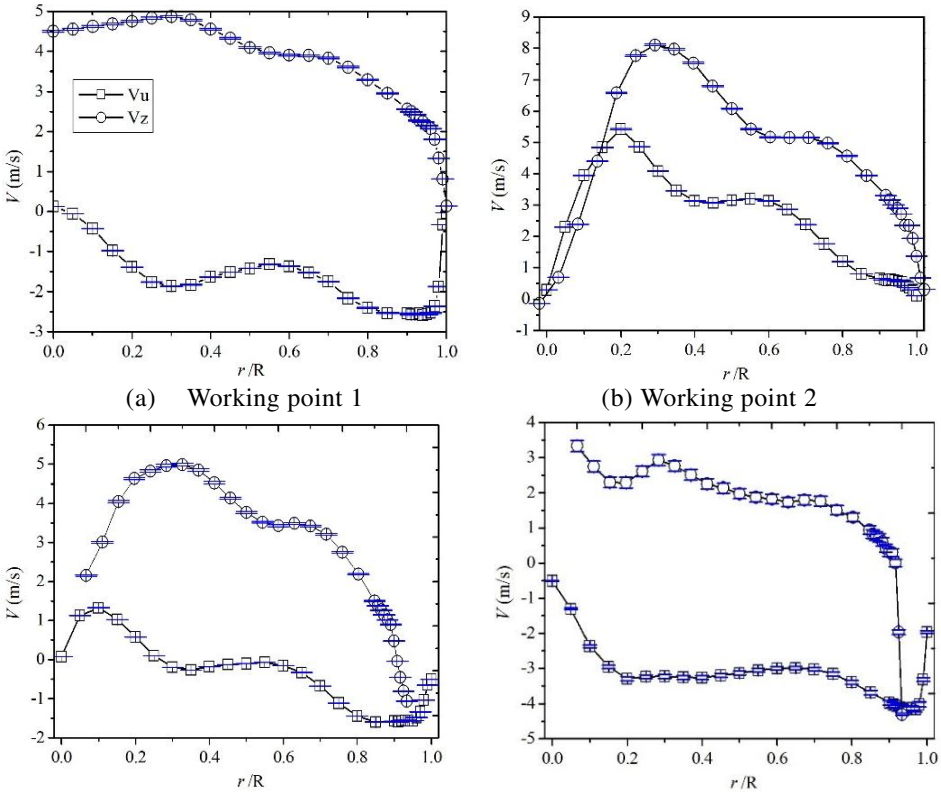

(a) Working point 1 (b) Working point 2

(c) Working point 3 (d) Working point 4

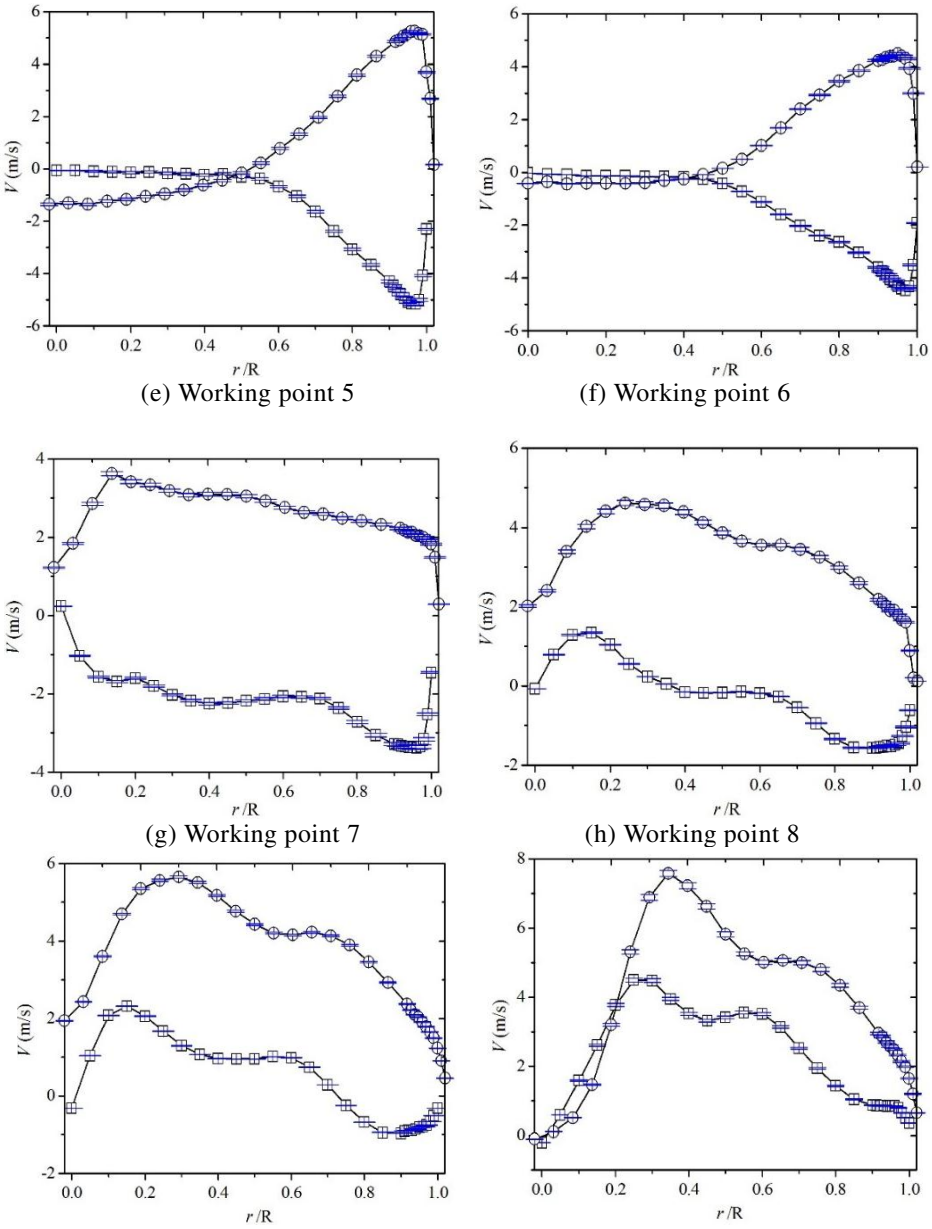

(e) Working point 5 (f) Working point 6

(g) Working point 7 (h) Working point 8

(i) Working point 9 (j) Working point 10

Figure 6. Tested velocity in the turbine mode at different working points (square line *V*u, circle line *V*z and blue line error bar).

In Figure 7, the distributions of circumferential velocity and axial velocity are very smooth at the working point 11 with the lowest head near the optimal point in the pump mode. The circumferential velocity and axial velocity distribution are increasing from 0 m/s to 5m/s and -5m/s from the centre to the wall of the draft tube at the working point 12, respectively. Near the centre, the velocity is nearly zero and the velocity is increasing quickly near the wall.

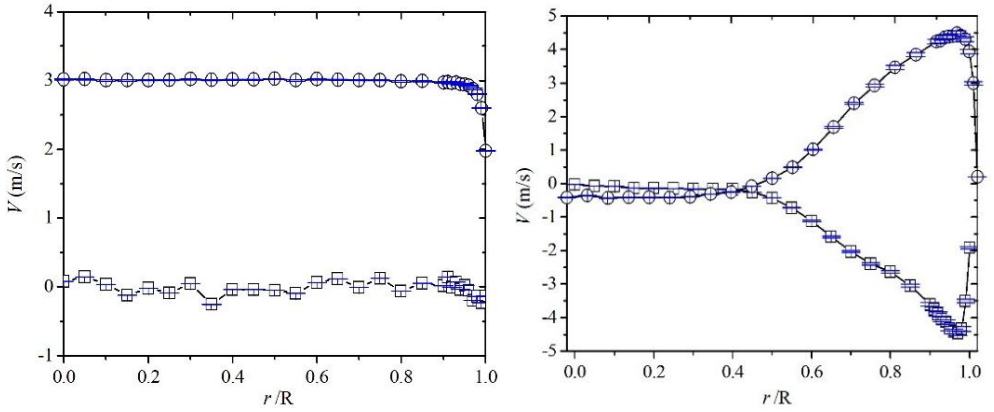

(a) Working point 11 (b) Working point 12

Figure 7. Tested velocity in the pump mode at different working points.

3.3 Flow field characteristics

The software ANSYSY was used to solve the unsteady flow governed by the incompressible Reynolds-averaged Navier-Stokes equations. A limited 2nd-order scheme was applied for the convection and diffusion terms. The mesh consists of the sub-domains of draft tube, impeller, guide vane, stay vane and spiral case in Figure 1. The grid has 5.5×10^6 node cells in total and the mesh detail is shown in Table 7. When the mesh number is 5×10^6, the comparison between simulation efficiency 0.920 and experimental value 0.918 has shown good agreement in Figure 8. The *k-ω* SST turbulence model with automatic wall treatment was applied for all simulations, which is well suited for ducted flows with adverse pressure gradients. The residual criterion for convergence is 0.0001.

Table 7. Mesh detail of pump-turbine.

	draft tube	impeller	guide vane	stay vane	spiral case
Node number(*10^6)	0.3	2.2	1.5	1.1	0.4
y^+	40	15	20	30	150
minimum skew angle(o)	35	52	54	32	22

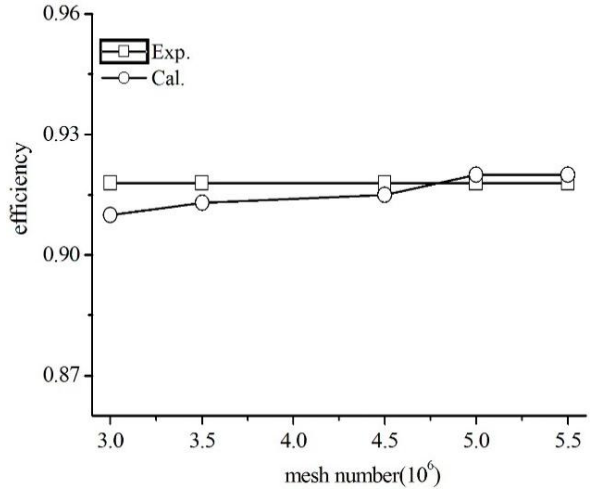

Figure 8. Calculated efficiency and mesh number.

The distribution of runner outlet velocity and the flow state are closely related to the runner. Figure 9 and 10 show the working condition 2, working condition 5, working condition 11 and working condition 12. The flow characteristics were analyzed at the working condition 2 with uniform velocity distribution which is better than that at the working condition 5 in the turbine mode. The flow distribution at the working condition 11 is better than that at the working condition 12. The velocity distribution at the working condition 12 is closely related to the pump hump phenomena. Some separation vortices exist at the runner inlet due to the blockage of the flow passage by the pump hump.

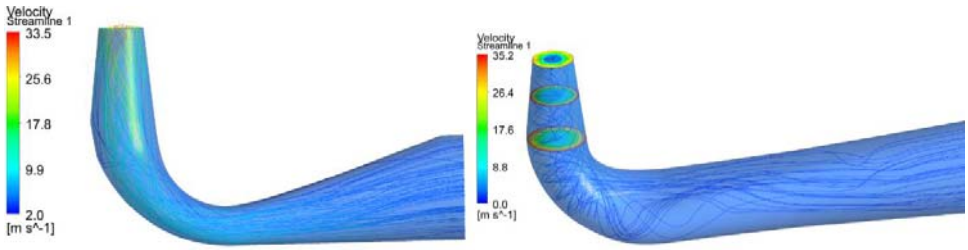

(a) Working condition 2 (b) Working condition 5

Figure 9. Streamlines at different working points in the turbine mode.

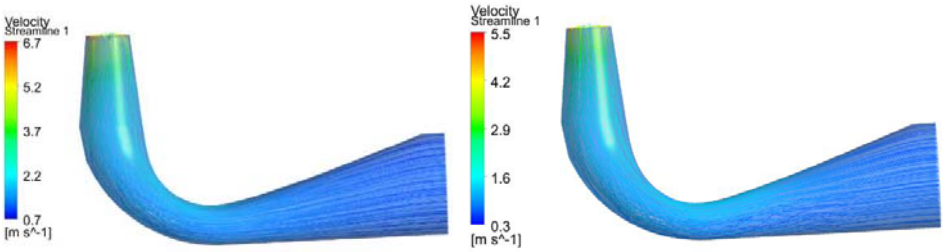

(a) Working condition 11 (b) Working condition 12

Figure 10. Streamlines at different working points in the pump mode.

By comparing the different velocity distributions at different working conditions, it can be seen that the calculated velocity distributions are similar to the tested results at the working points 1 and 11, as shown in Figure 11. The velocity testing by LDV is a validate method to test the velocity distribution.

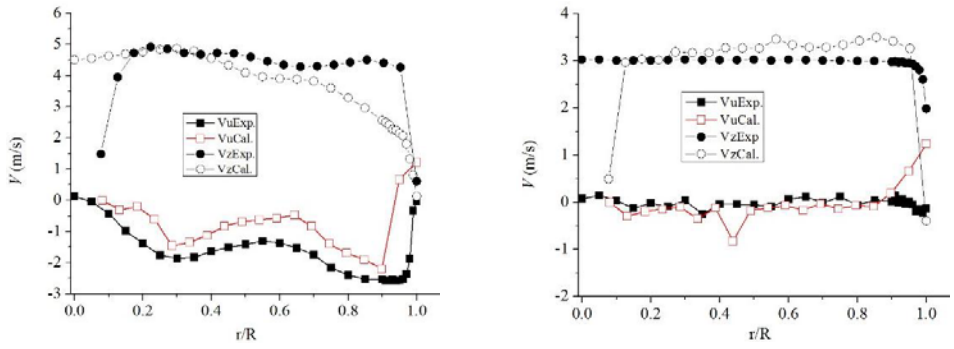

(a) Working condition 1 (b) Working condition 11

Figure11.Comparison of tested and calculated velocities.

4. Conclusions

The runner outlet velocity (turbine mode) or runner inlet velocity (pump mode) of the pump-turbine is

an important parameter affecting the performance of the unit. The velocity distribution at the runner outlet is tested by LDV, and the velocity characteristics are presented at different working conditions. The velocity characteristics are closely related to the flow in the runner, and the calculated velocity distribution is similar to the tested velocity.

5. Acknowledgments

The authors gratefully acknowledge the support from the Open Research Fund Program of State key Laboratory of Hydro science and Engineering (No. sklhse-2017-E-01)

References

[1] Lu, G., Zuo, Z., Sun, Y., Liu, D., Tsujimoto, Y., & Liu, S 2017 Experimental evidence of cavitation influences on the positive slope on the pump performance curve of a low specific speed model pump-turbine. *Renewable Energy,* p113.
[2] Nautiyal, H., Varun, & Kumar, A 2010 Reverse running pumps analytical, experimental and computational study: a review. *Renewable & Sustainable Energy Reviews,* **14**(7) pp 2059-67.
[3] Sheng, S 2002 New development in the technology of flow measurement over the last decade. *Mechanics & Engineering,* **24**(5) pp 1-14.
[4] Xiong, S 2014 A historical review for the 50~ (th) anniversary of laser doppler velocimetry. *Shiyan Liuti Lixue/journal of Experiments in Fluid Mechanics,* **28**(6) pp 51-5.
[5] Liu, Z. X., Yong, W., Cao, S. Z., Chuan-Gang, G. U., & Miao, Y. M 2004 LDV measurements of turbulent flow field in a centrifugal impeller at off-design flow. *Journal of Aerospace Power,* **19**(4), pp 449-54.
[6] Liu, Y. Z., Luo, C. S., & Chen, H. P 2002 Error analysis of the whole field velocity measurement results via LDV /PIV. *Journal of Shanghai Jiaotong University,* **36**(10) pp 1404-07.
[7] Lu, J 2000 Uncertainty investigation about the LDV calibration facility. *Chinese Journal of Scientific Instrument*.
[8] Li, G., Wu W., Zhang J., et al. Three-dimensional flow field structure of ship propeller analysis by means of 2D-LDV. *Acta Aero dynamica Sinica*, **32**(5) p 2014:0-0.
[9] Li, G. N 2010 LDV measurements of propeller trailing vortex. *Journal of Experiments in Fluid Mechanics*.
[10] Erne, S., Edinger, G., Maly, A., & Bauer, C 2017 Simulation and experimental investigation of the stay vane channel flow in a reversible pump turbine at off-design conditions. *Periodica Polytechnica Mechanical Engineering,* 61(No. 2 (2017)) pp 94-106.
[11] Zhang, Z 2011 Rotating stall mechanism and stability control in the pump flows. *Proceedings of the Institution of Mechanical Engineers, Part A: Journal of Power and Energy,* **225**(1) pp 779-88.
[12] Braun, O 2009 Part load flow in radial centrifugal pumps. *Epfl*.
[13] Favrel, A., Müller, A., Landry, C., Yamamoto, K., & Avellan, F 2016 Ldv survey of cavitation and resonance effect on the precessing vortex rope dynamics in the draft tube of Francis turbines. *Experiments in Fluids,* **57**(11) p 168.
[14] Müller, A., Favrel, A., Landry, C., Yamamoto, K., & Avellan, F 2017 Experimental Hydro-Mechanical Characterization of Full Load Pressure Surge in Francis Turbines. *Journal of Physics Conference Series* (Vol.**813**, p 012018). Journal of Physics Conference Series.
[15] Wang, H 2003 Experimental and numerical study of unsteady flow in a diffuser pump at off-design conditions. *Journal of Fluids Engineering,* **125**(5) pp 767-78.
[16] Magnoli M. V., Schilling R 2012 Numerical simulation of pressure pulsations in Francis Turbines. IOP Conference Series: *Earth and Environmental Science*.**15** (6) p 062029.
[17] Liu, J., Liu, S., Wu, Y., Jiao, L., Wang, L., & Sun, Y 2012 Numerical investigation of the hump characteristic of a pump–turbine based on an improved cavitation model. *The*

Constitution of the United States with case summaries /. Barnes & Noble Books.
[18] YIN J., WANG D., WANG L., & WEI X 2013 Advances in CFD flow simulations for pump-turbine. *Journal of Hydroelectric Engineering*, **32**(6) pp 233-238+243.